Incorporation Of Homogenizer In Nanoemulsion Injection Scheme For Enhanced Oil Recovery

Uchenna Odi*, Devon Energy, Houston, USA

Abstract

This work presents a theoretical approach of incorporating a homogenizer within a nanoemulsion injection scheme for enhanced oil recovery (EOR). Nanoemulsions are kinetically stable emulsions stabilized by surfactants with droplet sizes ranging from 20 to 500 nm and have the potential to deliver chemical agents depending on their application. For EOR, nanoemulsions have the potential to be more effective than the often used microemulsion which are thermodynamically stable and thus may break due to the heterogeneous conditions inherent in oil and gas reservoirs. There are two primary categories of nanoemulsion formulation which are high energy methods and low energy methods. High energy methods involve creating nanoemulsions using a high energy process such as high pressure homogenization. These methods can be expensive due to the energy applied to the nanoemulsion formulation process. Low energy methods involve manipulating the chemistry of the oil and surfactant formulation and are thus low cost due to the low energy input. Current technology illustrates that nanoemulsion size control is relatively straightforward using high energy methods such as high pressure homogenization.

Injecting incompressible fluids into a reservoir requires substantial energy in the form of pumps. Incorporating a homogenizer in the injection scheme gives an opportunity for the homogenizer to utilize the high energy inherent in the injection process. This is illustrated using the mechanical energy balance that combines the potential, kinetic, friction, and homogenizer pressure drops inherent in the incorporation of a homogenizer in the injection of nanoemulsions. Analysis shows the relative contributions of each of these pressure effects in the overall determination of the bottom hole injection pressure.

Incorporating a homogenizer into a nanoemulsion EOR process would schematically give direct control over nanoemulsion size while conserving energy by using the high energy inherent in an EOR injection process. This would be a novel direct approach of controlling the stability of nanoemulsions (by controlling the size) while not producing extra costs associated with high energy nanoemulsion creation methods. The describe procedure illustrates how to design an injection performance curve that can schematically give control of nanoemulsion size.

Introduction

Nanoemulsion EOR is an emerging smart fluid technology that has the potential to substantially increase ultimate recovery rates of reservoirs in the tertiary stages of recovery. Nanoemulsion formation is characterized as two methods which are high energy and low energy (Koreleva and Yurtov 2012). Low energy methods, which include phase inversion (by temperature or composition) and spontaneous emulsification, have been demonstrated but control of nanoemulsion diameter is not as straightforward as high energy methods. High energy methods which include high shear stirring, ultrasonic emulsification and high pressure homogenization are more energy intensive (and thus expensive) but give greater control of nanoemulsion diameter and therefore control of stability. A breakdown of nanoemulsion stability can be caused by gravitational separation (creaming/sedimentation), flocculation, coalescence, and Ostwald ripening (McClements 2012). Kinetic stability is critical to avoiding nanoemulsion breakage. Kinetic

stability of a nanoemulsion can be maintained as long as the energy barrier height between the nanoemulsion and separated state of the surfactant and oil mixture is greater than 20kT, where k is the Boltzman constant and T is the absolute temperature (McClements 2012). In addition, McClements has remarked that radius's less than 90 nm show ability to avoid gravitational separation (creaming/sedimentation) due to Brownian forces dominating gravitational forces.

Some authors have commented on the use of nanoemulsions for EOR. Del Gaudio et al. (2007) remarked on the potential application of nanoemulsions to deliver chemical agents that can increase oil recovery. In addition, Del Gaudio et al. were successful in creating several nanoemulsion formulations for EOR (Del Gaudio et al. 2013). Mandal et al. (2012) showed that nanoemulsions (consisting of mineral oil and a series of nonionic ethoxylated surfactants) in a core flood setup increased oil recovery up to 30% more after a water flood. Mandal et al. (2012) and Del Gaudio et al. (2007 and 2013) methods of nanoemulsion preparation were both categorized as low energy methods which have indirect control over nanoemulsion size. No authors have commented on the simultaneous injection of nanoemulsions of EOR while controlling nanoemulsion size. The original work here utilizes an existing nanoemulsion fluid and illustrates how to create injection performance curves that have the ability to control nanoemulsion size. Control of nanoemulsion size is essential for successful nanoemulsion EOR.

A high energy nanoemulsion system is presented in this work that utilizes the existing energy inherent in EOR injection to create and inject stable nanoemulsions. This process is verified by merging the theory of nanoemulsion creation into the mechanical energy balance of an EOR injection process. As examples, several nanoemulsion injection scenarios are presented that utilize this process using an example nanoemulsion, vertical well configuration, and several homogenizer dimensions.

Statement of Theory and Definitions

Consider the diagram in **Figure 1** which illustrates an injection scheme that is connected to a nanoemulsion formulation process which includes a mixing system, centrifugal pump and high pressure homogenizer. The first stage of this process is the mixing process. The purpose of the mixer is to create low energy emulsions by mixing the brine, surfactant, and oil phases together. In addition the mixer can also be used to mix already prepared nanoemulsions. After this mixing stage, the mixture is transported to the second stage by a centrifugal pump. The centrifugal pump pressurizes and transports the emulsion mixture to the third stage which is the high pressure homogenizer. The purpose of the homogenizer is to further reduce the nanoemulsion diameter to a desired value that ensures kinetic stability (radiuses less than 90 nm) (McClements 2012). After going through the homogenizer, the fluid is transported (still using the head of the centrifugal pump) to the fourth stage which is transport through the wellbore to the reservoir's sand face. As an assumption, every stage in the nanoemulsion injection process occurs at a steady state injection rate.

All four stages are linked and have an associated effect on one another. As an example, the emulsion diameter after the pumping stage can be large enough to warrant multiple passes through the homogenizer. Multiple passes through the homogenizer will reduce the overall bottom hole pressure. If the bottom hole pressure is less than the reservoir pressure than no injection can take place. Therefore, it is important to consider emulsion size in conjunction with a mechanical energy balance so that the bottom hole injection pressure is above the reservoir pressure.
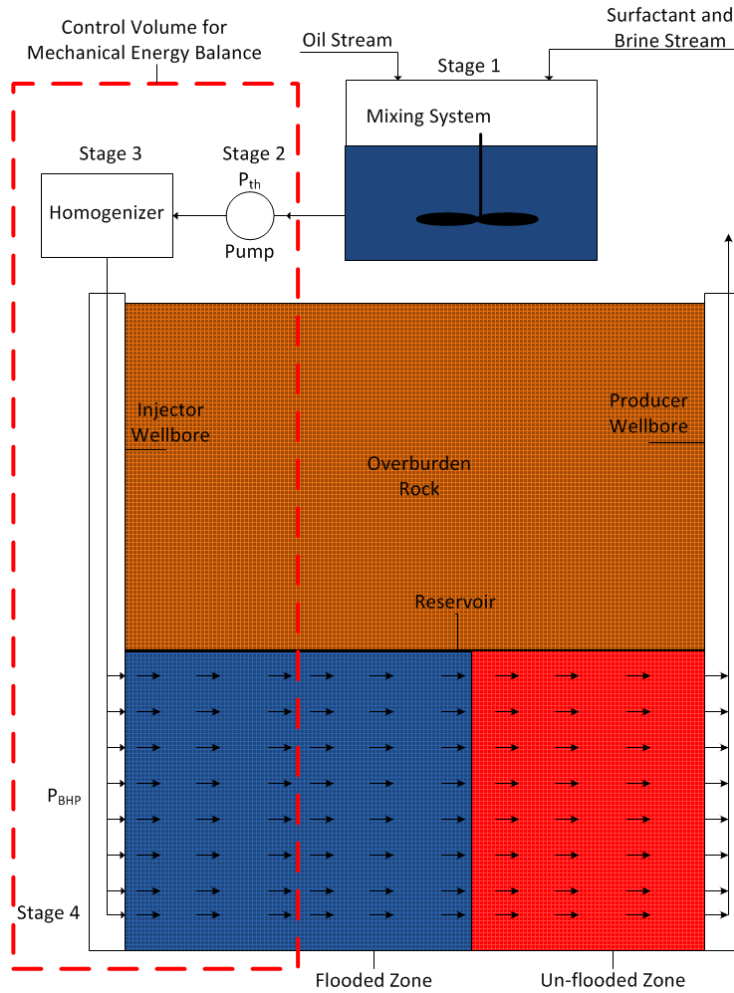
Figure 1—Nanoemulsion injection system.

Nanoemulsion Size Control. The emulsion mixture goes through several processes that have the ability to impart energy in various forms which may have wide implications on nanoemulsion size. The primary difference in each of the processes is the turbulent energy of dissipation. Each process imparts a form of energy onto the emulsion. For the mixer, it has been remarked that the turbulent energy of dissipation is in the order of 10-100 W/kg (Davis 1987). This range is miniscule when compared to homogenizers and other high energy methods which are 10^8 W/kg and greater (Davis 1987). Davis (1987) proposed a widely used expression for emulsion diameter as a function of the turbulent energy of dissipation and emulsion properties. The expression for emulsion diameter, d_{ne}, is conveyed in the following relationship.

$$d_{ne} = \left(\frac{4}{C_1 C_2}\right)^{3/5} \left(1 + \left(\frac{\sqrt{C_2}}{4}\right)\frac{\mu_D \varepsilon^{1/3} d_{ne}^{1/3}}{\sigma}\right)^{3/5} \left(\sigma^{3/5} \rho_C^{-3/5} \varepsilon^{-2/5}\right), \dots\dots\dots\dots\dots\dots\dots\dots\dots\dots\dots\dots\dots(1)$$

where C_1 and C_2 are constants equal to 0.7 and 2 respectively; μ_D is the dispersed phase viscosity; ε is the turbulent energy of dissipation; ρ_C is the density of the continuous phase; and σ is the interfacial tension between the oil and aqueous phases. The turbulent energy of dissipation is the key factor in controlling the nanoemulsion diameter. Using Davis's equation and assuming the physical properties of a typical emulsion, it is possible to see the relationship between the energy of dissipation and emulsion droplet size. This relationship is expressed in the following figure for emulsions where the continuous phase density is approximately 1000 kg/m^3 and the interfacial tension is .001 N/m.
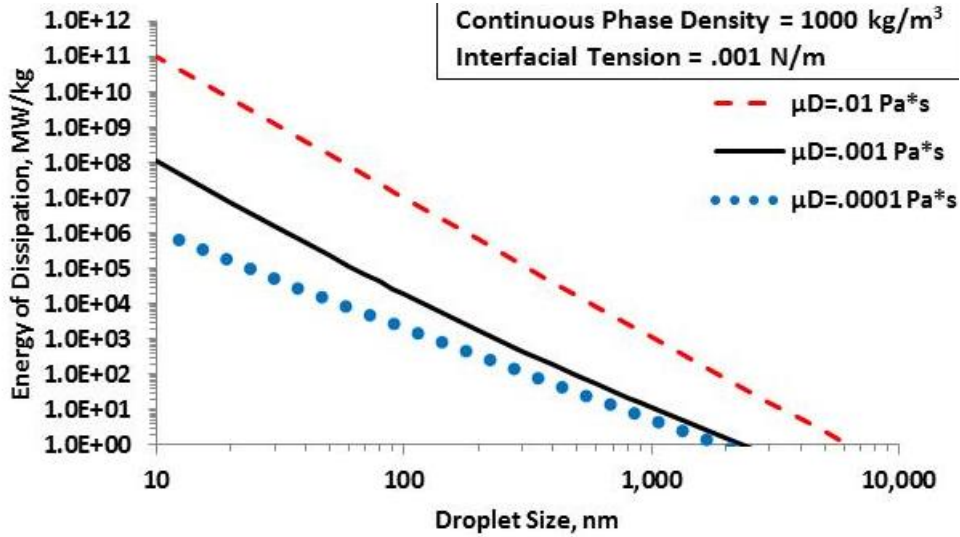
Figure 2—Turbulent energy of dissipation as a function of emulsion droplet size using Davis's expression.

Figure 2 (in diameter length scales) illustrates that stable nanoemulsions (radiuses less than 90 nm or 180 nm diameter) can be made using turbulent energy of dissipations greater than approximately 5×10^3 MW/kg for dispersed phase viscosities of approximately .001 Pa*s. To make stable nanoemulsions with an increased dispersed phase viscosity of .01 Pa*s, results in a required turbulent energy of dissipation of approximately 3×10^6 MW/kg or greater. To make stable nanoemulsions with a decreased dispersed phase viscosity of .0001 Pa*s, results in a required turbulent energy of dissipation of approximately 7×10^2 or greater. These results indicate that amount of energy needed to reduce emulsion size substantially increases as the dispersed phase viscosity increases. Additionally, these results show that the energy of dissipation can be used to directly control nanoemulsion size.

For a homogenizer, the energy of dissipation can be directly controlled using the dimensions of the homogenizer. These dimensions are illustrated in **Figure 3**.
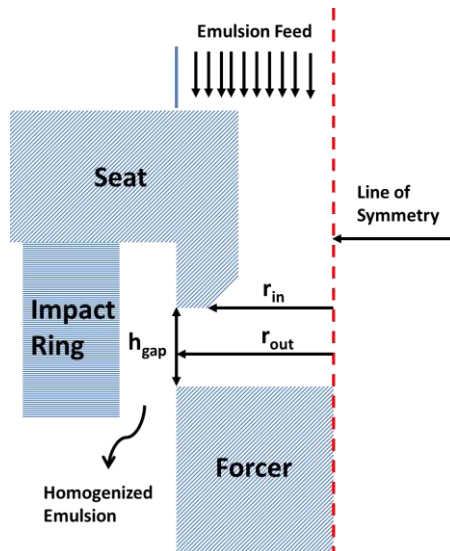

Figure 3—Homogenizer valve cross section (rotate along axis of symmetry for complete cross section, not drawn to scale).

Using this active zone, the energy of dissipation for the homogenizer is the following (Hakansson 2007).

$$\varepsilon_H = \frac{\Delta P_H Q}{\pi(r_{out}^2 - r_{in}^2)h_{gap}\rho_M};\dots\dots\dots\dots\dots\dots\dots\dots\dots\dots\dots\dots\dots\dots\dots\dots\dots(2)$$

Where r_{in} is the homogenizer inlet radius, r_{out} is the homogenizer outlet radius, h_{gap} is the gap height of the

homogenizer, Q is the volumetric flow rate of emulsion, ρ_M is the density of the emulsion, and ΔP_H is the pressure drop through the homogenizer. Several homogenizers placed in series is equivalent to multiple passes through one homogoenzier. The energy of dissipation for N passes through the homogenizer is derived to be the following (see Appendix).

$$\varepsilon_H = \frac{N\Delta P_H Q}{\pi(r_{out}^2 - r_{in}^2)h_{gap}\rho_M},\dots\dots\dots\dots\dots\dots\dots\dots\dots\dots\dots\dots\dots\dots\dots(3)$$

Observing the expressions for the energy of dissipation from one pass in the homogenizer and N passes through a homogenizer, it is evident that the total turbulent energy of dissipation is directly proportional to the number of passes or number of identical homogenizers in series. When several homogenizers are placed in series together, the equivalent total energy of dissipation can be found by substituting the energy of dissipation for each individual homogenizer. This results in the following expression for the total energy of dissipation.

$$\varepsilon_H = \varepsilon_{H_1} + \varepsilon_{H_2} + \cdots + \varepsilon_{H_N} = \sum_{i=1}^{N}\varepsilon_{H_i},\dots\dots\dots\dots\dots\dots\dots\dots\dots\dots\dots\dots(4)$$

This result states that for identical homogenizers in series, the total energy of dissipation is the summation of their respective turbulent energies of dissipation. This conclusion can be extended to multiple emulsion droplet reducing machines in series. The sum of their turbulent energies of dissipations can be used to effectively determine resulting droplet size. As an example, consider an emulsion with properties listed in **Figure 4** that undergoes several passes using a homogenizer with specifications listed in Figure 4. This emulsion's size is simulated in Figure 4 as a function of number of passes in the homogenizer. A decay relationship, first proposed by Hatton et al. (2014) described the eventual decline of emulsion size as the number of passes. This relationship is described in the following expression.

$$d_{ne} = d_\infty + A_n e^{-N/N_b},\dots\dots\dots\dots\dots\dots\dots\dots\dots\dots\dots\dots\dots\dots(5)$$

Where A_n is a parameter in the fit, N_b is the number of passes until emulsion breakage and d_∞ is the emulsion size after an infinite amount of passes. The parameter A_n can be quantified by understanding that before the emulsion enters the homogenizer, the parameter N_H is 0. Therefore, $d_{ne} = d_\infty + A_n$ which is essentially the initial emulsion diameter size before homogenization. Figure 4 illustrates this best fit line using the previous relationship and the simulated data.
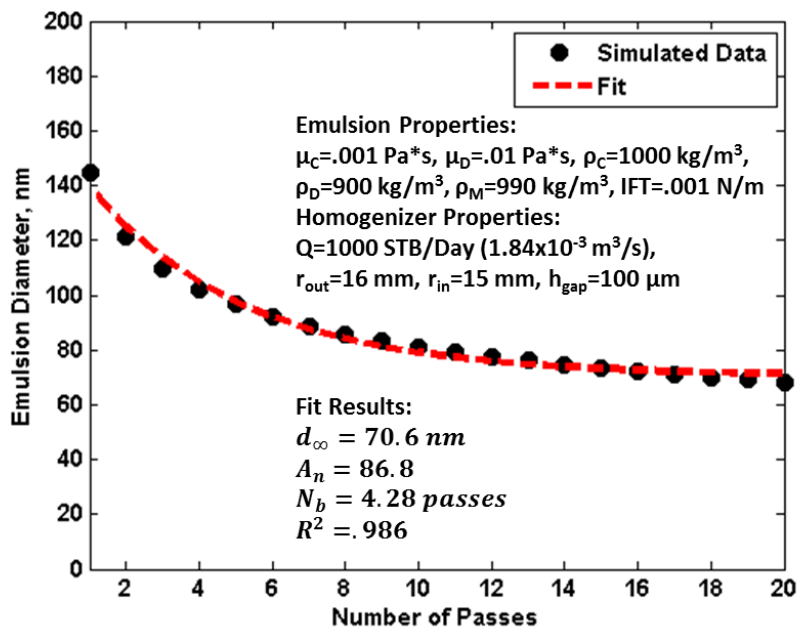

Figure 4—Simulated emulsion as a function of homogenizer passes.

Because the sum of the turbulent energy of dissipations is the total contribution of the energy imparted onto the emulsion, the emulsion diameter is then a function of the total turbulent energy of dissipation along with the specific properties of the emulsion. For the Nanoemulsion Injection System, the total energy of dissipation can be modeled using the following expression.

$$\varepsilon_T = \varepsilon_M + \varepsilon_{CP} + \varepsilon_H, \dots\dots\dots\dots\dots\dots\dots\dots\dots\dots\dots\dots\dots\dots\dots\dots\dots\dots\dots\dots\dots\dots\dots\dots\dots\dots\dots(6)$$

Where ε_M is the turbulent energy of dissipation for the mixer, ε_{CP} is the turbulent energy of dissipation for the centrifugal pump, and ε_H is the turbulent energy of dissipation for the homogenizer(s). The starting point of the nanoemulsion injection system is the mixer. The turbulent energy dissipation for a mixer is function of the impeller diameter and impeller speed. The expression for the turbulent energy of dissipation in a mixer is represented in the following expression (Morales et al. 2013).

$$\varepsilon_M = \kappa_M N_M^3 L_M, \dots\dots\dots\dots\dots\dots\dots\dots\dots\dots\dots\dots\dots\dots\dots\dots\dots\dots\dots\dots\dots\dots\dots\dots\dots\dots\dots(7)$$

Where κ_M is the mixing turbulent energy of dissipation for the mixer, N_m is the mixing impeller angular velocity, and L_m is the mixing impeller diameter. The mixing system used in this work has the general ability to mix the aqueous and oil phases for pressurization through the centrifugal pump. All specifications for the mixing system are listed in **Table 1**.

Table 1—Mixing system specifications.

Mixing Impeller Diameter	.232 m
Mixing Turbulent Energy of Dissipation	0.0019
Mixing Impeller Angular Velocity	150 RPM

To determine the emulsion size as a result of passing through a centrifugal pump requires quantifying the turbulent energy of dissipation for the centrifugal pump. The turbulent energy dissipation for a centrifugal pump is a function of the hydraulic power performed on the fluid. Specifically, it can be represented using the following expression (Morales et al. 2013).

$$\varepsilon_{CP} = \kappa_{CP} \frac{\Delta P_{CP} Q}{\rho_M V_{CP}}, \dots\dots\dots\dots\dots\dots\dots\dots\dots\dots\dots\dots\dots\dots\dots\dots\dots\dots\dots\dots\dots\dots\dots\dots(8)$$

Where κ_{CP} is the fraction of total dissipated energy by turbulence for the centrifugal pump, ΔP_{CP} is the change in pressure caused by the centrifugal pump and V_{CP} is the volume of the centrifugal pump. Using the previous expression and the Davis expression for emulsion diameter, it is possible to estimate the emulsion size as a result of pumping the emulsion product from the mixing system through the centrifugal pump. The resulting high pressured emulsion from the centrifugal pump is the premix feed into the high pressure homogenizer. Emulsion size can be further controlled by using the homogenizer's ability to pass the emulsion mixture through several homogenizer passes. It is possible to incorporate emulsions size control in the injection scheme of nanoemulsions by performing a mechanical energy balance on the nanoemulsion injection system.

Description and Application of Equipment and Processes

The injection bottom hole pressure is a function of the fluid changes due to the pump, potential energy, kinetic energy, and friction (with full discussion in the Appendix). A homogenizer can be added to this conventional setup by adding another pressure drop attributed to N passes through the homogenizers in series. Quantitatively this pressure drop is $N\Delta P_H$. The bottom hole pressure from the mechanical energy balance across an injection system incorporating a homogenizer is then represented using the following equation.

$$P_{BHP} = P_{th} + \Delta P_{PE} - \Delta P_{KE} - \Delta P_f - N_H \Delta P_H, \dots\dots\dots\dots\dots\dots\dots\dots\dots\dots\dots\dots\dots\dots\dots\dots(9)$$

Where P_{th} is the pressure contribution due to the pump, ΔP_{PE} is the pressure drop due to potential energy, ΔP_{KE} is the pressure drop due to kinetic energy, and ΔP_f is the pressure drop due to friction. Using the previous expression, nanoemulsion size control can be incorporated into the mechanical energy balance. The primary challenge in implementing the nanoemulsion injection scheme is ensuring that there is enough pressure to inject and enough turbulent energy of dissipation to control the nanoemulsion size. These goals are counterintuitive because ensuring emulsion radiuses of 90 nm or less (for stability) requires large turbulent energies of dissipation which correspondingly require large pressure drops through the

homogenizers. Large pressure drops through multiple homogenizers would reduce the bottom hole injection pressure to values less than the reservoir pressure which would result in nanoemulsion injection failure. Conversely, only ensuring bottom hole pressures larger than the reservoir pressure would result in small pressure drops in the homogenizers which would then result in low turbulent energies of dissipation. Radiuses greater than 90 nm would then be created and would cause nanoemulsion failure because these diameters are outside the stable nanoemulsion class. A generalized algorithm can be created that ensures that nanoemulsions with radiuses less than 90 nm (diameter less than 180 nm) are created with sufficient pressure for injection against a reservoir pressure, P_{resv}.

Illustrated in **Figure 5**, this algorithm shows that for a limit of N_{limit} homogenizers in series it is possible to create stable nanoemulsions by systematically going through a three step checklist after each homogenizer pass. After each homogenizer pass, this checklist consists of first verifying if $N\Delta P_H < P_{th}$ is true. If $N\Delta P_H < P_{th}$ is false than there can be no injection of nanoemulsion. If $N\Delta P_H < P_{th}$ is true then the second point on the checklist, $d_{ne} \leq 180$ nm, needs to be checked. If the second point, $d_{ne} \leq 180$ nm, is false then the emulsion needs another pass through a homogenizer. If $d_{ne} \leq 180$ nm is true then the third point on the checklist, $P_{BHP} > P_{resv}$, needs to be checked. If the third point, $P_{BHP} > P_{resv}$, is false than there can be no injection of nanoemulsion. If $P_{BHP} > P_{resv}$ is true, than there is successful nanoemulsion injection. Applying this algorithm for a desired nanoemulsion injection rate, it is possible to create stable nanoemulsions with sufficient injection pressure.
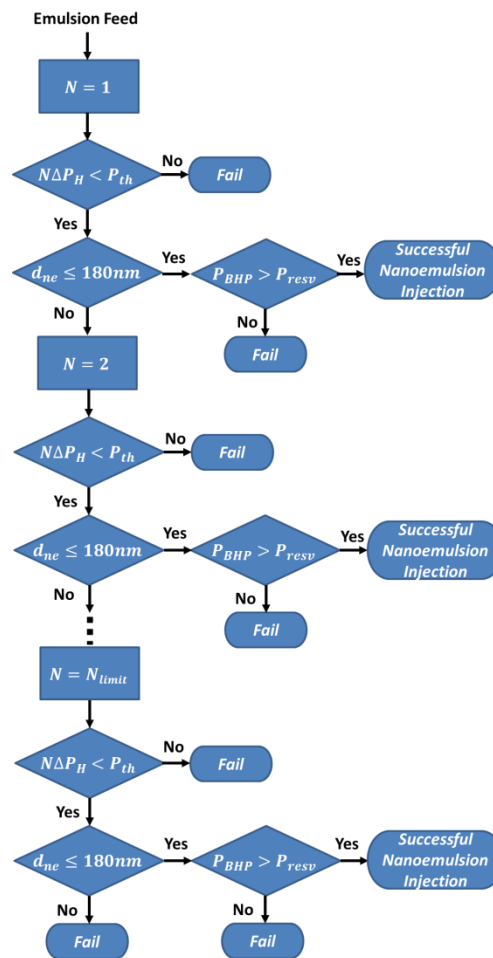

Figure 5—Generalized nanoemulsion injection algorithm.

Proper homogenizer dimensions can be used to mitigate the two conflicting goals of nanoemulsion injection and nanoemulsion size control. Homogenizer dimensions can do this by creating enough turbulent energy of dissipation to reduce emulsion diameter at moderate homogenizer pressure drops that minimize the deduction from the bottom hole injection pressure. To adequately compare homogenizer performance, Innings and Tragardh (2007) proposed dimensionless groups and length scales which are represented in the

following expressions.

$$N_{Re,Gap} = \frac{\rho_M Q}{2\pi r_{out}\mu_M},\dots\dots\dots\dots\dots\dots\dots\dots\dots\dots\dots\dots\dots\dots\dots\dots\dots\dots\dots\dots\dots\dots\dots\dots(10)$$

$$N_{G,Kol} = \frac{h_{Gap}}{\eta},\dots\dots\dots\dots\dots\dots\dots\dots\dots\dots\dots\dots\dots\dots\dots\dots\dots\dots\dots\dots\dots\dots\dots\dots\dots\dots\dots(11)$$

$$\eta = \left(\frac{\mu_M}{\rho_M\varepsilon}\right)^{\frac{1}{4}},\dots\dots\dots\dots\dots\dots\dots\dots\dots\dots\dots\dots\dots\dots\dots\dots\dots\dots\dots\dots\dots\dots\dots\dots\dots(12)$$

$$l_0 = \eta \cdot N_{Re,Gap}^{\frac{3}{4}},\dots\dots\dots\dots\dots\dots\dots\dots\dots\dots\dots\dots\dots\dots\dots\dots\dots\dots\dots\dots\dots\dots\dots\dots\dots(13)$$

Where $N_{Re,Gap}$ is the gap Reynolds number, $N_{G,Kol}$ is the turbulent gap height, η is the Kolmogorov length scale, and l_0 is the largest eddy scale. These groups can be used to compare the performance of different homogenizer dimensions. They will also give insight on homogenizer dimensions that are essential to successful nanoemulsion injection.

Presentation of Data and Results

To illustrate the effectiveness of the Nanoemulsion Injection system a Tween 80/Span 80 and diesel fuel nanoemulsion injection is simulated using nanoemulsion experimental data from Noor El-Din et al. (2013). Specifically, this system is a water in oil nanoemulsion that contains 9 wt% water and 10 wt% active surfactants (53.3wt% Tween 80 and 46.7wt% Span 80) in the aqueous phase and diesel fuel as the oil phase. Noor El-Din et al. (2013) measured the HLB of the aqueous phase as 10, the critical micelle concentration of the mixed surfactant system as 14.3×10^{-4} mol/L, and the interfacial tension between the oil and aqueous phase at the critical micelle concentration as 3.8 mN/m. Noor El-Din et al. (2013) also measured the density and kinematic viscosity of the nanoemulsion system for different volume fractions of the aqueous phase illustrated in **Figure 6** and **Figure** 7. Using the density and kinematic viscosity as functions of temperature, dynamic viscosity values were determined as a function of temperature. As previously discussed, nanoemulsion viscosity and density are critical parameters in the calculation of the bottom-hole injection pressure. These parameters are essential in quantifying viscosity and density changes caused by temperature increases in the injection tubing as the nanoemulsion is transported from the homogenizer and through the wellbore to the reservoir's sand face.
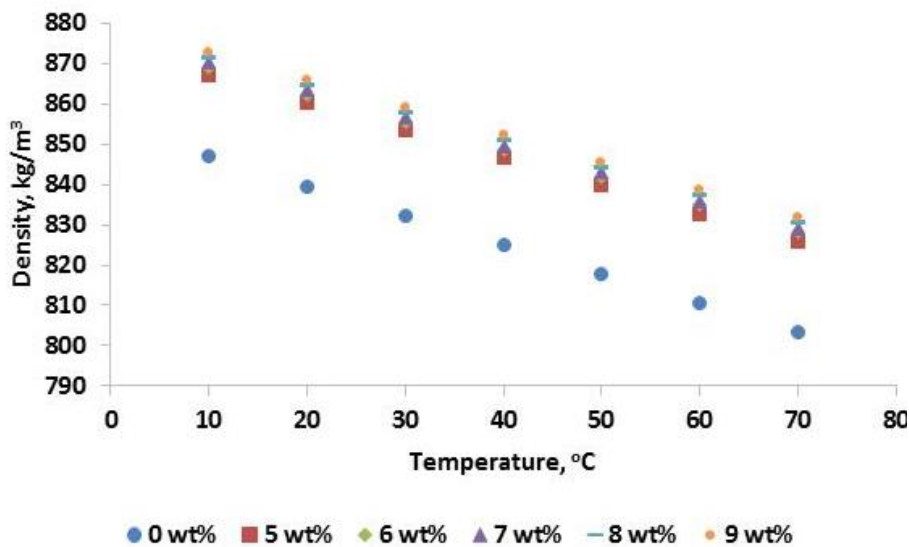

Figure 6—0-9 wt% Water and 10 wt% Surfactant Mixture (53.3 wt% Tween 80 and 46.7 wt% Span 80) in Diesel Nanoemulsion Density as Function of Temperature (Noor El-Din et al. 2013).
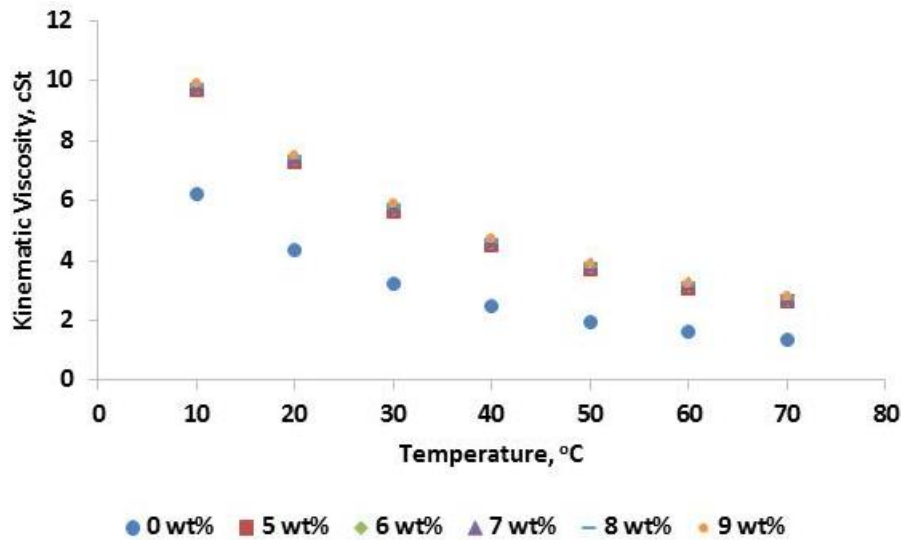
Figure 7—0-9 wt% Water and 10 wt% Surfactant Mixture (53.3 wt% Tween 80 and 46.7 wt% Span 80) in Diesel Nanoemulsion Kinematic Viscosity as Function of Temperature (Noor El-Din et al. 2013).

Noor El-Din et al. (2013) experimental nanoemulsion diameter was measured as 49.55 nm and was obtained using a high pressure homogenizer. For this work, 49.55 nm is the target diameter because it represents the minimum diameter obtained experimentally. Using this target diameter, Noor El-Din's emulsion properties, and a test injection rate of 1000 STB/day (159 m^3/day), homogenizer gap heights were determined for four cases of homogenizer dimensions. Homogenizer gap heights were determined by first solving for the turbulent energy of dissipation for a diameter equal to 49.55 nm. From there, the turbulent energy of dissipation was used along with user defined homogenizer inlet and outlet radiuses to solve for the gap height in the homogenizer turbulent energy of dissipation expression. Using this procedure, gap heights were determined for four homogenizer dimensions labeled accordingly in the following table along with their characteristic properties.

Observing **Table 2**, it is apparent that the pressure drop is reduced for the same turbulent energy of dissipation as the homogenizer dimensions progress from Production Scale to the 2nd Proposed Nano Scale. This is an important result because it shows that the homogenizer pressure drop can be reduced without adversely affecting the homogenizer's ability to produce nanoemulsions. In addition, turbulence is increased as the homogenizer dimensions progress to the 2nd Nano Scale which may be an indication that more energy is utilized in the process of reducing the emulsions diameter.

A vertical well configuration with a target reservoir temperature of 99°C (210°F) and other parameters listed in **Table 3** was used to illustrate the nanoemulsion injection system. Using the vertical well configuration, several homogenizer scenarios indicated in Table 2 were simulated.

Table 2—Homogenizer Dimensions (d_{ne}=49.55 nm, Q=1000 STB/Day (159 m^3/Day), Temp.=60°F (15.6°C)).

	Production Scale	Pilot Scale	1st Proposed Nano scale	2nd Proposed Nano scale
r_{out}, mm	16	4	2	1
r_{in}, mm	15	3	1	0.5
h_{gap}, µm	170	291	413	696
ΔP_H, MPa	5,290	2,050	1,250	524
ε, MW/kg	677,000	677,000	677,000	677,000
$N_{Re,Gap}$	2,140	8,570	17,200	34,300
η, µm	59.6	59.6	59.6	59.6
l_0, mm	18.8	53.1	89.3	150.2
$N_{G,Kol}$	2.85	4.89	6.93	11.7

Table 3—Well parameters.

Pipe Roughness	0.0006
Tubing Inner Diameter	0.0762 m (3 inches)
Surface Temperature	15.6°C (60°F)
Geothermal Gradient	8.33°C per 304.8 m, (15°F per 1000 ft)
Injection Tubing Length	3048 m (10000 ft)
Inclination Angle	90°
Total Depth	3048 m (10,000 ft)
Change in Depth	3.048 m (10 ft)

The results of these simulations are illustrated in **Figure 8** through **Figure** 11. Observing the pressure contributions illustrated in Figure 8, it is apparent that the bottom hole injection pressure increases for the same nanoemulsion injection rate as the homogenizer dimensions progress from Production Scale to the 2nd Proposed Nano Scale. This occurs primarily because the pressure drop due to homogenization is minimized as the homogenizer dimensions progress from the Production Scale to the 2nd Proposed Nano Scale. A reduction of the homogenizer pressure drop ensures larger range of positive bottom hole injection pressures.
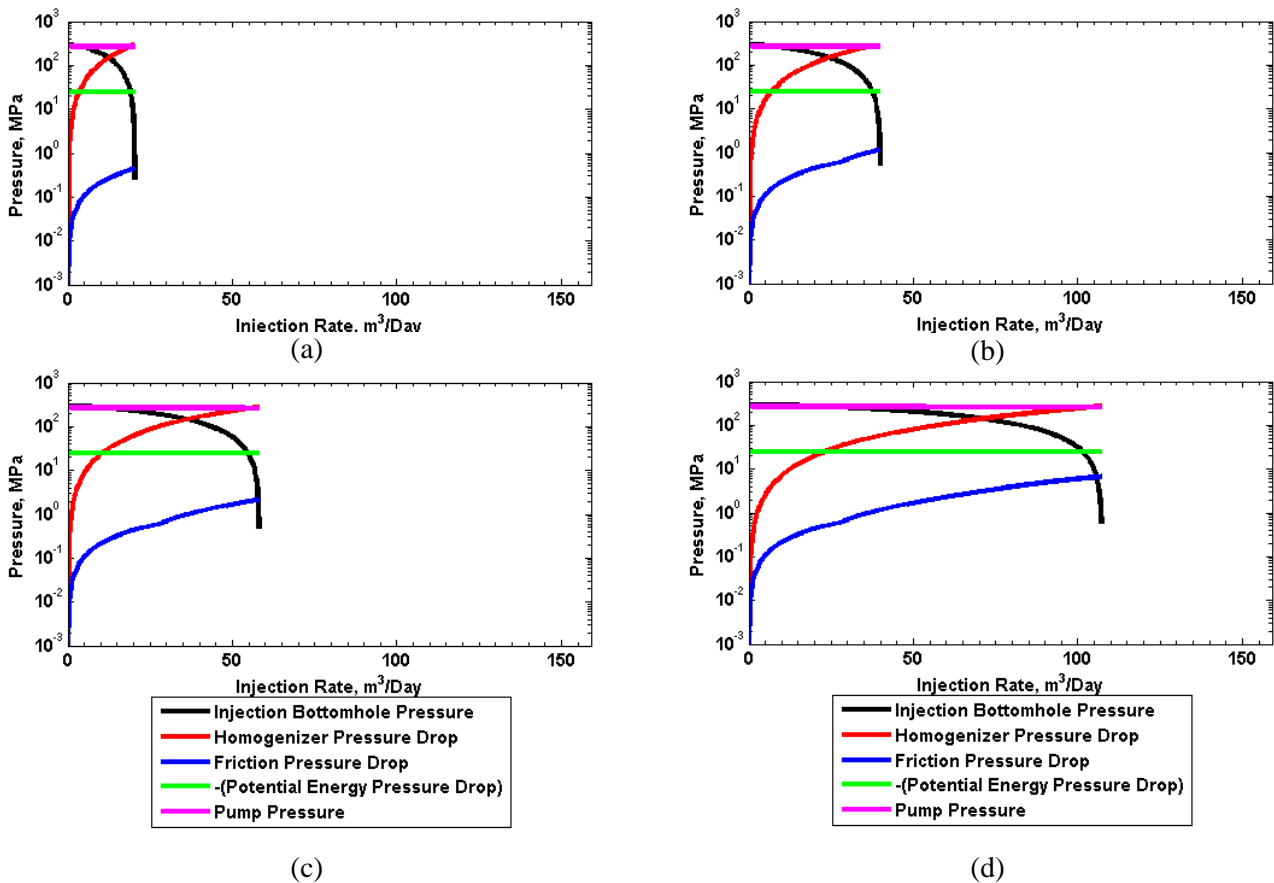

Figure 8—Bottom Hole Pressure and Pressure Drops for N_{limit} = 1 (a) Production Scale (b) Pilot Scale (c) 1st Proposed Nano Scale (d) 2nd Proposed Nano Scale.
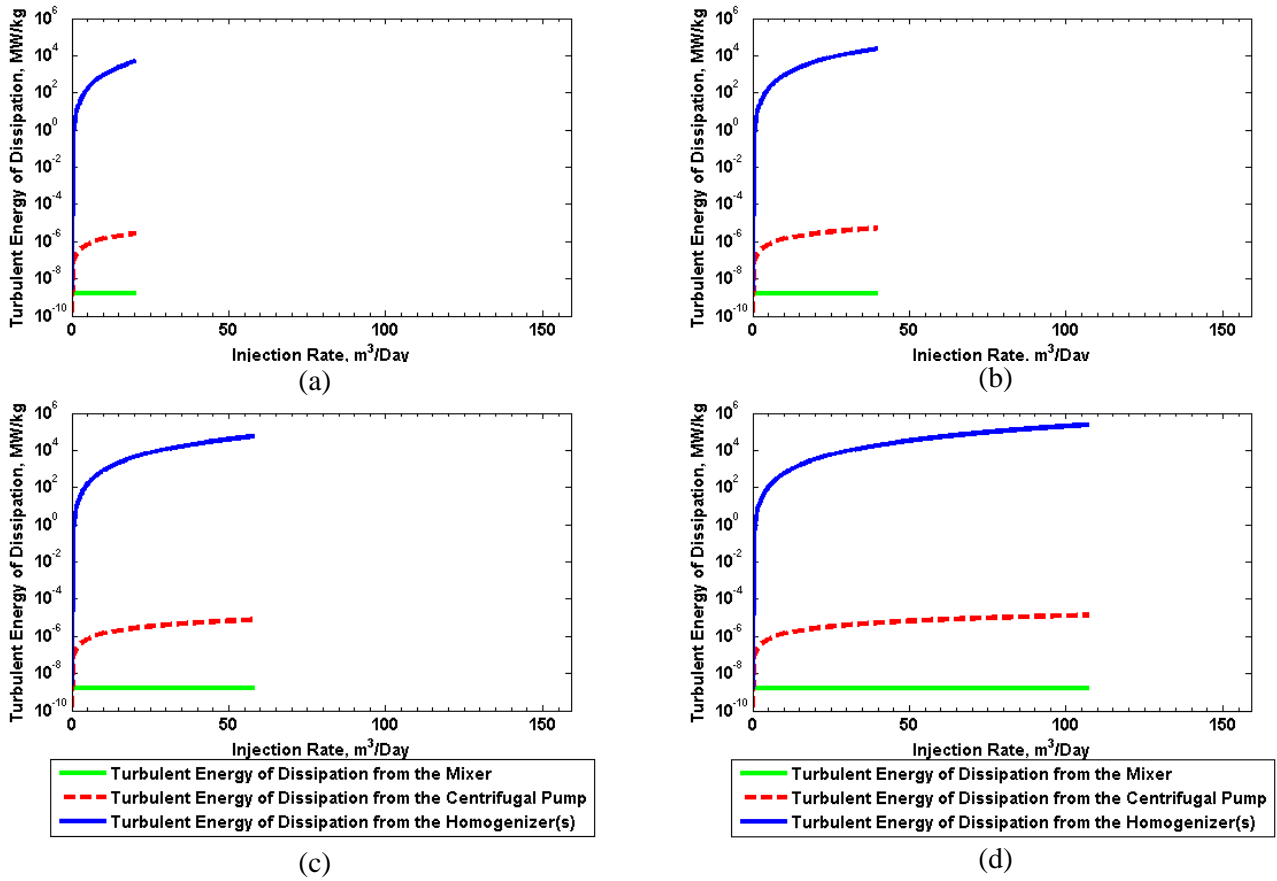
Figure 9—Turbulent Energy of Dissipation for $N_{limit} = 1$ (a) Production Scale (b) Pilot Scale (c) 1st Proposed Nano Scale (d) 2nd Proposed Nano Scale.

As a consequence of extending the bottom hole pressure over a larger range of injection rates for specific homogenizer dimensions, there is a larger range of turbulent energies of dissipation and thus a larger range of emulsion diameters. This is portrayed in **Figure 9** and **Figure** 10 which show that as the homogenizer dimensions progress from the Production Scale to the 2nd Proposed Nano Scale there is larger amount of energy dissipated in the creation of smaller diameter emulsions.

Observing all the presented homogenizer dimensions, it is apparent that the 2nd Proposed Nano Scale had the largest impact on emulsion diameter reduction. The injection range in which positive injection pressures and kinetically stable emulsion diameters occurred for this homogenizer was an injection flow rate of 32 m^3/Day at a bottom hole injection pressure of 251 MPa to an injection flow rate of 107 m^3/Day at a bottom hole injection pressure of 0.585 MPa.

When compared to the 2nd Proposed Nano Scale, the other homogenizer specifications did not have the same success in reducing the emulsion diameters as conveyed by **Table 4**. Overall, all of the homogenizers exhibited the same trend of having the emulsion diameters decrease. This decrease was limited by the homogenizer pressure drop. Because of this, it is essential to choose the right homogenizer dimensions so as to ensure stable nanoemulsions and adequate nanoemulsion injection.

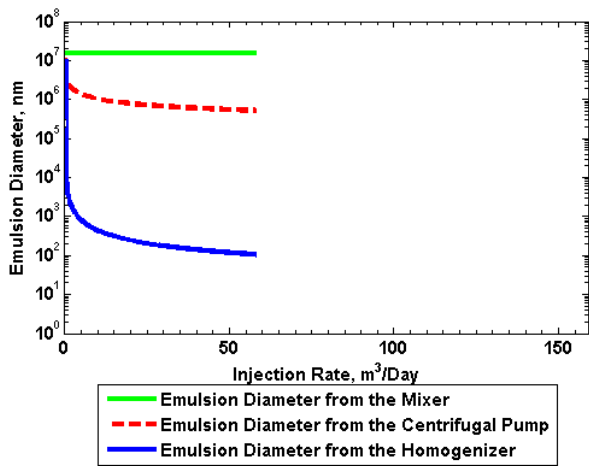**Table 4—Minimum Diameters Obtained for Nanoemulsion Injection.**

	Minimum Diameter, nm	Injection Rate at Minimum Diameter, m3/Day	Bottom Hole Pressure at minimum Diameter, MPa
Production Scale	235	20.2	0.259
Pilot Scale	138	39.7	0.530
1st Proposed Nano Scale	105	58.0	0.492
2nd Proposed Nano Scale	67.8	107	.585
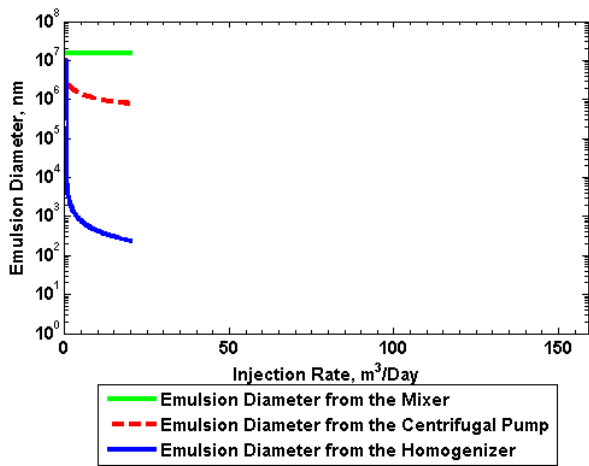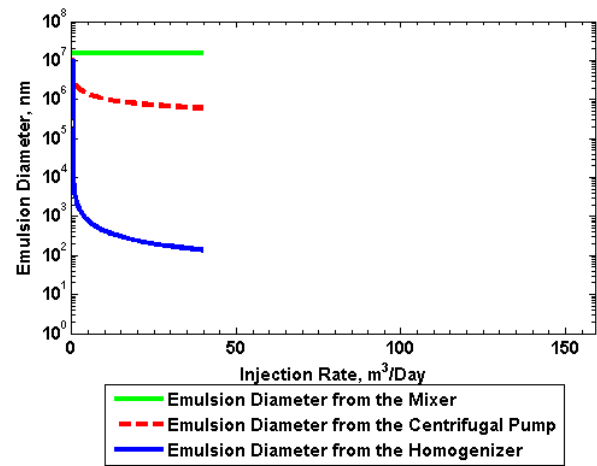
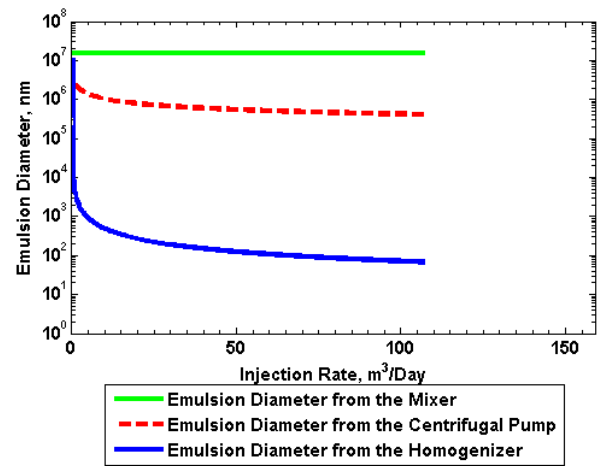**Figure 10—Emulsion Diameter for $N_{limit} = 1$ (a) Production Scale (b) Pilot Scale (c) 1st Proposed Nano Scale (d) 2nd Proposed Nano Scale.**

In addition to the homogenizer dimension study presented earlier, an additional study was conducted to see if adding homogenizers in series according to the algorithm presented in Figure 5 is beneficial. This scenario was conducted using the dimensions of the 2nd Proposed Nano Scale. The emulsion diameter results are illustrated in **Figure 11**. These results show that increasing the amount of homogenizers results in no beneficial decrease in nanoemulsion diameter. This occurs because increasing the amount of homogenizers correspondingly increases the total homogenizer pressure drop. Increasing the total homogenizer pressure limits the bottom hole injection pressure range which thus reduces the injection rate range of how far the emulsion diameter can be reduced.
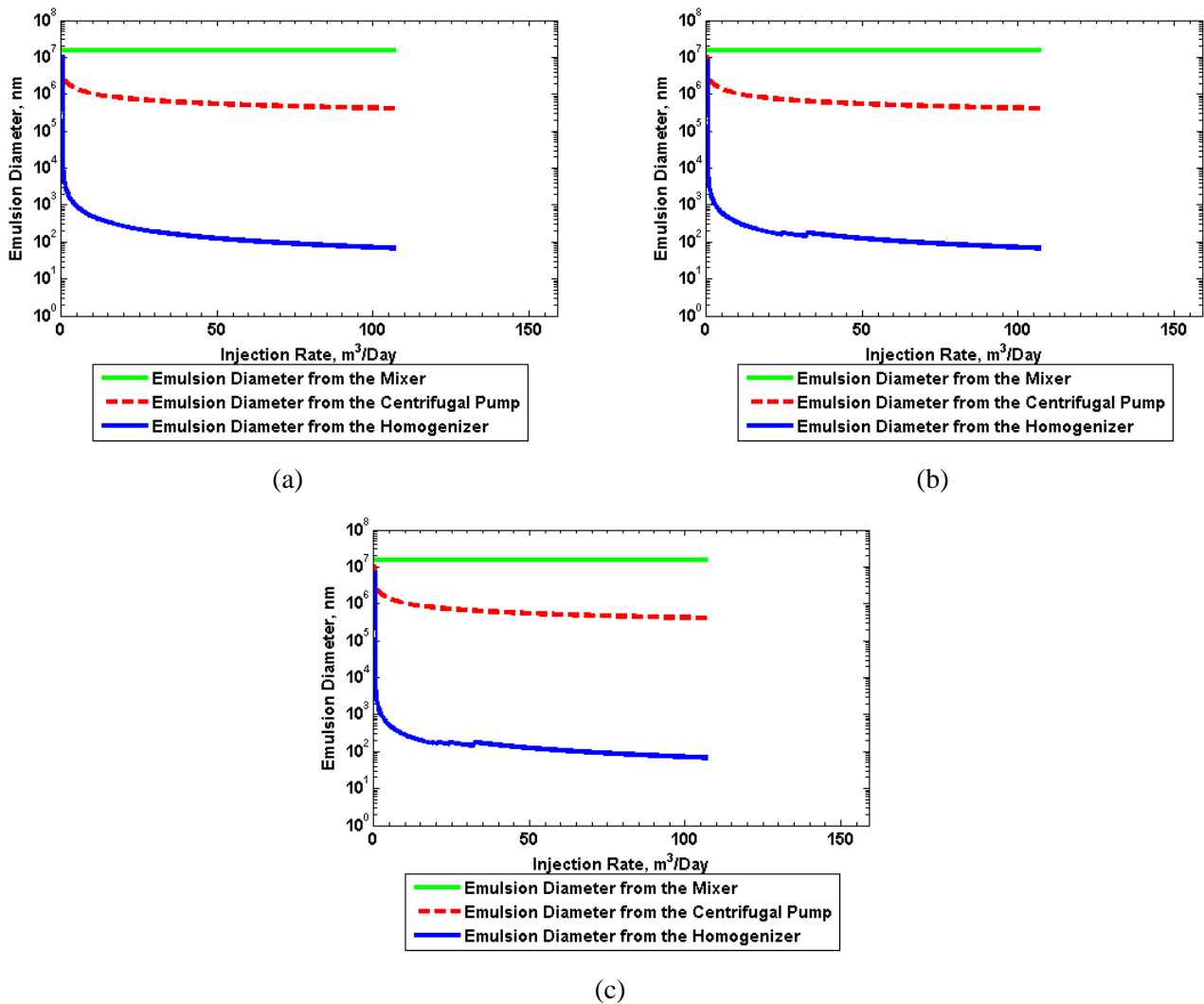
(a)

(b)

(c)

Figure 11—Diameter using 2nd Proposed Nano Scale (a) N$_{limit}$=1, (b) N$_{limit}$=3, (c) N$_{limit}$=5.

Economics

Equipment and transportation costs are the primary differences between onsite and offsite production of nanoemulsions for the oil field. Onsite production of nanoemulsions which utilizes a homogenizer incorporated into an EOR injection scheme requires capital investment due to homogenizers, mixers, and centrifugal pumps. While a single homogenizer and single mixer could be sized accordingly to service several wells in a field (estimated total capital cost ranging from 1-10 million USD), the cost of several centrifugal pumps for injection depends on the number of wells in a field. Because of this, the total cost of the nanoemulsion injection system depends on the number of wells utilized in the field. The final decision to use the onsite option depends on if the capital costs of the onsite implementation are less than the transportation costs to deliver offsite produced nanoemulsions.

Regardless of the choice between onsite and offsite options, the one similarity between these two options is the chemical cost associated with creating the nanoemulsion. Nanoemulsions fundamentally contain oil, water, and surfactants. Considering these components it is possible to determine the chemical cost per volume of a nanoemulsion by utilizing the following equation.

$$C_{NE} = \rho_M \left(\frac{f_{m,W} C_W}{\rho_W} + f_{m,S} C_S + f_{m,O} C_O \right), \dots\dots\dots\dots\dots\dots\dots\dots\dots\dots\dots\dots\dots\dots\dots\dots\dots\dots\dots(14)$$

Where $f_{m,W}$ is the mass fraction of water in the nanoemulsion, C_W is the cost per volume of water, ρ_W is the density of water in the nanoemulsion, $f_{m,S}$ is the mass fraction of surfactants in the nanoemulsion, C_S is the cost per mass of surfactants in the nanoemulsion, $f_{m,O}$ is the mass fraction of oil phase in the nanoemulsion, and C_O is the cost per mass of oil in the nanoemulsion. Considering the nanoemulsion investigated in this

13

work and the chemical costs of each component the nanoemulsion costs is approximately $5.98 per liter. This costs is relatively expensive due to the expensive cost of surfactants (Tween 80 is $114 per gallon, Span 80 is $96.20 per liter) and diesel (3.65 per gallon). In addition, the majority of the investigated nanoemulsion is diesel by mass. These costs are lab scale and can be further reduced using carefully selected suppliers or cheaper chemical substitutes when scaled up to field use. To ensure profitability for the nanoemulsion injection system, the current commodity price of oil must be more than the cost of delivering the nanoemulsion to the reservoir.

When considering the numerous possible nanoemulsions (water in oil and oil in water) it is possible to determine the range of chemical cost associated with nanoemulsion formulation by using MonteCarlo simulation. These simulation results using the uniform distributed parameters in **Table 5** and a range of 800 kg/m^3 to 1200 kg/m^3 for the nanoemulsion density gives a nanoemulsion cost ranging from $.0044 to $21.62 per liter. Additional specifics regarding the possible nanoemulsion costs are illustrated in **Figure 12**.
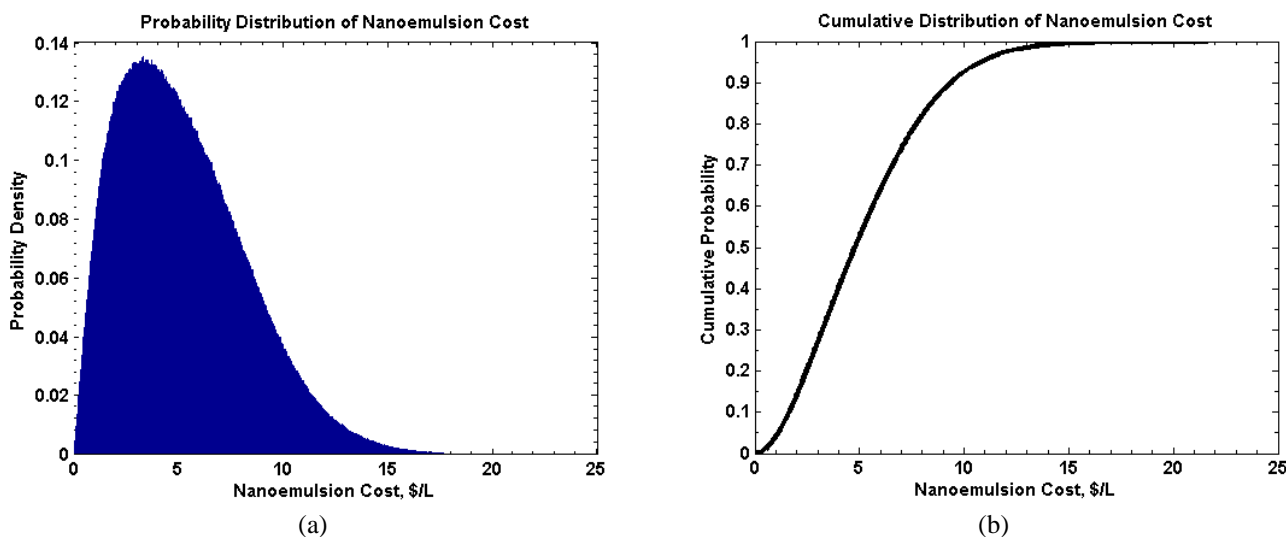

(a)   (b)

Figure 12—Results of MonteCarlo Simulation of Nanoemulsion Cost (a) Probability Distribution Function (b) Cumulative Distribution Function.

Table 5—Parameters for montecarlo simulation of nanoemulsion cost.

	Water Phase	Surfactant Phase	Oil Phase
Minimum Mass Fraction	.01	.01	.01
Maximum Mass Fraction	.90	.10	.98
Minimum Density	1000	-	-
Maximum Density	1200	-	-
Minimum Cost	$.01 per barrel	$.01 per kg	$.01 per kg
Maximum Cost	$10 per barrel	100 per kg	10 per kg

These results show that it is important to have low cost surfactants and low cost oil. Having low cost nanoemulsion components ensures that the margin between nanoemulsion chemical cost and oil price is large enough to justify nanoemulsion EOR.

Conclusions

It is theoretically possible to create nanoemulsions within an EOR injection scheme. Proof of this concept is accomplished by incorporating the production of nanoemulsions into the mechanical energy balance. Successful nanoemulsion injection is strongly dependent on the homogenizer dimensions. Inadequate homogenizer dimensions cause too much of a pressure drop or too small of an energy of dissipation. Proper

homogenizer dimensions have adequate pressure drops with substantial turbulent energies of dissipation that reduce the emulsion to stable nanoemulsion sizes. Utilizing the 2nd Proposed Nano Scale, it is possible to combine the production of nanoemulsions into a nanoemulsion injection scheme.

Acknowledgement

Conflicts of Interest

The author(s) declare that they have no conflicting interests.

References

Del Gaudio, L., Bortolo, R., and Lockhart, T. P. 2007. Nanoemulsions: A New Vehicle for Chemical Additive Delivery. Paper presented at the 2007 SPE International Symposium on Oilfield Chemistry. Houston, TX, 28 February-2 March. SPE-106016-MS.

Del Gaudio, L., Lockhart, T. P., Belloni, A., et al. 2013. Process for the Preparation of Water-in-Oil and Oil-in-Water Nanoemulsions. U.S. Patent Application 13/845,515, filed March 18, 2013.

Economides, M. J., Hill, A. D., and Ehlig-Economides, C. 1994. *Petroleum Production Systems*. Englewood Cliffs, N.J.: PTR Prentice Hall.

Hakansson, A. 2007. Dynamic Modelling of High Pressure High Pressure Homogenizer. Master Thesis. Department of Food Technology, Engineering and Nutrition. Lund University, Sweden.

Hakansson, A., Tragardh, C., and Bergenstahl, B. 2009. Dynamic Simulation of Emulsion Formation in a High Pressure Homogenizer. *Chemical Engineering Science* **64**(12):2915-2925.

Hatton, T. A., Doyle, P. S., Doyle, G. A., et al. 2014. Nanoemulsions: Mechanistic Evaluation of Formation, Stability and Applications. Massachusetts Institute of Technology.

Innings, F. and Tragardh, C. 2007. Analysis of the Flow Field in a High-Pressure Homogenizer. *Experimental Thermal and Fluid Science* **32**(2):345-354.

Mandal, A., Bera, A., Ojha, K., et al. 2012. Characterization of Surfactant Stabilized Nanoemulsion and Its Use in Enhanced Oil Recovery. Paper presented at the 2012 SPE International Oilfield Nanotechnology Conference. Noordwijk, The Netherlands, 12-14 June. SPE-55406-MS.

McClements, D. J. 2012. Nanoemulsions Versus Microemulsions: Terminology, Differences, And Similarities. *Soft Matter* **8**(3):1719-1729.

Morales, R., Pereyra, E., Wang, S., et al. 2013. Droplet Formation Through Centrifugal Pumps for Oil-Water Dispersions. *SPE Journal* **18**(2013):172- 178. SPE-163055-PA.

Noor El-Din, M. R., El-Hamouly, S. H., Mohamed, H. M., et al. 2013. Water-in-Diesel Fuel Nanoemulsions: Preparation, Stability, and Physical Properties. *Egyptian Journal of Petroleum* **22**(2013):517-530.

The MathWorks. 2014. Centrifugal Pump. http://www.mathworks.com/help/physmod/hydro/ref/centrifugalpump.html?refresh=true.

Appendix

Energy of Dissipation through a Homogenizer Derivation. The energy of dissipation using the homogenizer dimensions can be quantified by assuming that the major fragmentation and coalescence occurs in the gap just after the Seat and before the Forcer as a consequence of the pressure drop through the gap. Using this active zone, the energy of dissipation for the homogenizer is the following (Hakansson 2007).

$$\varepsilon_H = \frac{\Delta P_H Q}{\pi (r_{out}^2 - r_{in}^2) h_{gap} \rho_M}, \dots\dots\dots\dots\dots\dots\dots\dots\dots\dots\dots\dots\dots\dots\dots\dots(A1)$$

Where r_{in} is the homogenizer inlet radius, r_{out} is the homogenizer outlet radius, h_{gap} is the gap height of the homogenizer, Q is the volumetric flow rate of emulsion, ρ_M is the density of the emulsion, and ΔP_H is the pressure drop through the homogenizer expressed as the following (Hakansson et al. 2009).

$$\Delta P_H = \frac{\rho_C}{4}\left(\frac{Q}{2\pi r_{in} h_{gap}}\right)^2 + \frac{5\rho_C \mu_C^{3/5} Q^{7/5}}{(2\pi)^{7/5} h_{gap}^3}\left(\frac{1}{r_{in}^{2/5}} + \frac{1}{r_{out}^{2/5}}\right) + \frac{\rho_C}{2}\left(\frac{Q}{2\pi r_{out} h_{gap}}\right)^2 \dots\dots\dots\dots\dots\dots\dots\dots(A2)$$

Substituting the pressure drop expression in the turbulent energy of dissipation expression results in the following expression which illustrates that the turbulent energy of dissipation is a function of the homogenizer dimensions which are r_{in}, r_{out}, and h_{gap}.

$$\varepsilon_H = \left(\frac{\rho_C}{4}\left(\frac{Q}{2\pi r_{in}h_{gap}}\right)\right)^2 + \frac{5\rho_C\mu_C^{3/5}Q^{7/5}}{(2\pi)^{7/5}h_{gap}{}^3}\left(\frac{1}{r_{in}{}^{2/5}}+\frac{1}{r_{out}{}^{2/5}}\right) + \frac{\rho_C}{2}\left(\frac{Q}{2\pi r_{out}h_{gap}}\right)^2\left(\frac{Q}{\pi(r_{out}^2-r_{in}^2)h_{gap}\rho_M}\right)\dots\dots(A3)$$

Ideally, it is desired to create nanoemulsions after one pass in the homogenizer. However it may not be possible to do this depending on the dimensions of the homogenizer. Because of this, it is important to model the homogenizer for N passes. This can be done by first considering homogenizers with the same dimensions in series as illustrated in **Figure 13a**. These homogenizers have the same pressure drop through them ($\Delta P_{H_1} = \Delta P_{H_2} = \cdots = \Delta P_{H_N}$) and therefore have the same turbulent energy of dissipation ($\varepsilon_{H_1} = \varepsilon_{H_2} = \cdots = \varepsilon_{H_N}$). Effectively, this means that each homogenizer has the same ability to change emulsion size.
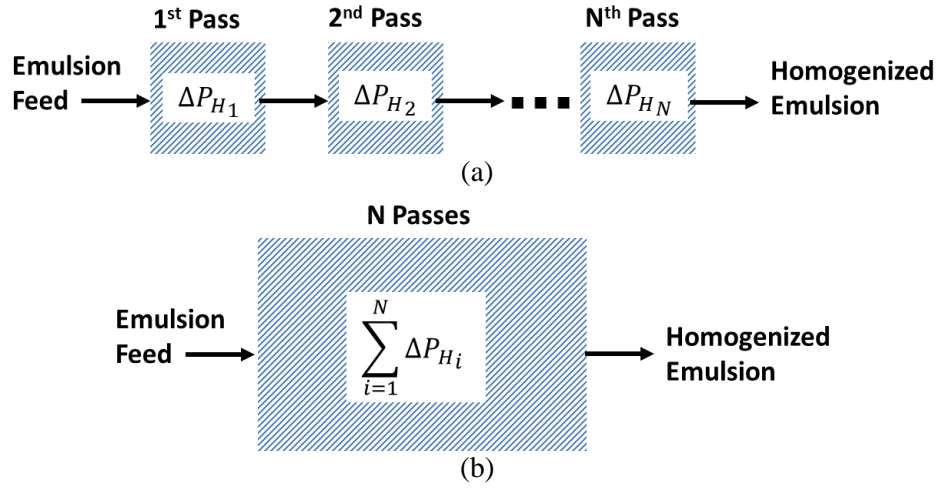

(a)

(b)

Figure 13—Pressure Drops in a Series of Homogenizers (a) Individual in Series (b) Summation of Individual in Series.

As the emulsion passes through each homogenizer, it has a pressure drop equal to the summation of pressure drops as illustrated in **Figure 13b**. Using the analogy presented in the previous figure, it is possible to deduce the total turbulent energy of dissipation as a result of passing through a series of these homogenizers. This expression is derived by starting with the expression for turbulent energy of dissipation and the total pressure drop through the homogenizer.

$$\varepsilon_H = \frac{Q}{\pi(r_{out}^2-r_{in}^2)h_{gap}\rho_M}\left[\Delta P_{H_1} + \Delta P_{H_2} + \cdots + \Delta P_{H_N}\right]\dots\dots\dots(A4)$$

Multiplying out the pressure drop terms results in the following expression.

$$\varepsilon_H = \frac{\Delta P_{H_1}Q}{\pi(r_{out}^2-r_{in}^2)h_{gap}\rho_M} + \frac{\Delta P_{H_2}Q}{\pi(r_{out}^2-r_{in}^2)h_{gap}\rho_M} + \cdots + \frac{\Delta P_{H_N}Q}{\pi(r_{out}^2-r_{in}^2)h_{gap}\rho_M}\dots\dots(A5)$$

There are two conclusions that can be made from the previous expression. Since $\Delta P_H = \Delta P_{H_1} = \Delta P_{H_2} = \cdots = \Delta P_{H_N}$, there are N pressure drops with a pressure drop of ΔP_H. Therefore, the total pressure drop through the system of homogenizers is $N\Delta P_H$. Using this statement, the first conclusion is the final expression for the turbulent energy of dissipation for N homogenizers in series.

$$\varepsilon_H = \frac{N\Delta P_H Q}{\pi(r_{out}^2-r_{in}^2)h_{gap}\rho_M}\dots\dots(A6)$$

Mechanical Energy Balance. Nanoemulsion injection is possible when the bottom hole injection pressure (P_{BHP}) at the reservoir's sand face is greater than the pressure in the reservoir. The bottom hole injection pressure is determined by first performing an energy balance on the injection system which includes everything downstream from the pump to the sand face of the reservoir system. The following equation describes the energy balance for a production/injection system (Economides et al. 1994) excluding a homogenizer.

16

$$\frac{dP}{\rho_M} + \frac{udu}{g_c} + \frac{g}{g_c}dz + \frac{2f_f u^2 dL}{g_c D} + dW_s = 0,\dots\dots\dots\dots\dots\dots\dots\dots\dots\dots\dots\dots\dots\dots\dots\dots\dots\dots\dots(A7)$$

where P corresponds to pressure, u is the injection velocity, z is the height from the injection site to the reservoir's sand face, f_f is the friction factor, D is the wellbore diameter, and W_s is the shaft work. Integrating the previous equation from the injection site (Stage 2) to the reservoir's sand face (Stage 4) and solving for the total pressure drop leaves the following expression.

$$\Delta P = \Delta P_{PE} - \Delta P_{KE} - \Delta P_f\dots\dots\dots\dots\dots\dots\dots\dots\dots\dots\dots\dots\dots\dots\dots\dots\dots\dots\dots\dots..(A8)$$

The total pressure drop, ΔP, is the pressure loss experienced from transporting a fluid from the pump to the reservoir's sand face (without a homogenizer). This pressure drop is the sum of pressures which include the pressure increase due to the weight of fluid (ΔP_{PE}, potential energy), the pressure loss due to decreasing the diameter of flow (ΔP_{KE}, kinetic energy), and the pressure loss due to friction (ΔP_f). It is possible to determine each of these contributions by first dividing the length of the wellbore into N_L segments with each segment being of length dL. The pressure drop due to kinetic energy in a section of pipe can be determined using the following relationship.

$$\Delta P_{KE} = \frac{8Q^2}{\pi^2 g_c}\sum_{i=1}^{N_L}\rho_{Mi}\left(\frac{1}{D_i^4} - \frac{1}{D_{i-1}^4}\right)\dots\dots\dots\dots\dots\dots\dots\dots\dots\dots\dots\dots\dots\dots\dots\dots..(A9)$$

The parameter i corresponds to the ith segment along the length of the wellbore. The pressure drop due to potential energy can be determined using the following relationship.

$$\Delta P_{PE} = \frac{g}{g_c}\sum_{i=1}^{N_L}\rho_{Mi}dL_i \sin\theta_i\dots\dots\dots\dots\dots\dots\dots\dots\dots\dots\dots\dots\dots\dots\dots\dots\dots\dots\dots.(A10)$$

The parameter Θ is the angle of well inclination. The pressure drop due to friction can be determined using the following relationship.

$$\Delta P_f = \frac{2}{g_c}\sum_{i=1}^{N_L}\frac{\rho_{Mi}f_{fi}u_i^2 dL_i}{D_i}\dots\dots\dots\dots\dots\dots\dots\dots\dots\dots\dots\dots\dots\dots\dots\dots\dots\dots\dots\dots.(A11)$$

The fanning friction factor, f_f, for the ith segment can be determined by first calculating the Reynolds Number (N_{Re}) illustrated in the following expression (Economides et al., 1994).

$$N_{Re} = \frac{\rho_M u D}{\mu_M},\dots\dots\dots\dots\dots\dots\dots\dots\dots\dots\dots\dots\dots\dots\dots\dots\dots\dots\dots\dots\dots\dots\dots\dots...(A12)$$

where μ_M is the viscosity of the nanoemulsion mixture. Using the Reynolds Number, the fanning friction factor can be calculated using the laminar ($N_{Re} \leq 2100$) or turbulent ($N_{Re} > 2100$) flow regimes (Economides et al. 1994).

$$f_f = \begin{cases} \dfrac{16}{N_{Re}} & \text{for } N_{Re} \leq 2100 \\[2em] \left[-4\log\left(\dfrac{\varepsilon_R}{3.7065} - \dfrac{5.0452}{N_{Re}}\log\left(\dfrac{\varepsilon_R^{1.1098}}{2.8257} + \left(\dfrac{7.149}{N_{Re}}\right)^{0.8981}\right)\right)\right]^{-2} & \text{for } N_{Re} > 2100 \end{cases},\dots\dots\dots\dots.(A13)$$

The parameter, ε_R, is the relative pipe roughness. Incorporating the pressure contribution due to the pump (P_{th}) it is possible to determine the bottom hole injection pressure, P_{BHP}, using the following relationship.

$$P_{BHP} = P_{th} + \Delta P_{PE} - \Delta P_{KE} - \Delta P_f\dots\dots\dots\dots\dots\dots\dots\dots\dots\dots\dots\dots\dots\dots\dots\dots..(A14)$$

The pressure contribution due to the pump can be determined by using a pumping curve (for a centrifugal pump) and common affinity laws that scale pump performance as a function of required injection rate (Mathworks 2014). These affinity laws can be utilized by first relating the required injection rate, Q, and the pumps impeller angular velocity, ω, to the rate provided by the pumping curve, Q_{curve}, and the pumping curve's angular velocity, ω_{curve}. This relation is expressed as the following equation.

$$Q_{curve} = Q\left(\frac{\omega_{curve}}{\omega}\right)\dots\dots\dots\dots\dots\dots\dots\dots\dots\dots\dots\dots\dots\dots\dots\dots\dots\dots\dots\dots...(A15)$$

The pressure contribution due to the pump can then be determined by first finding its equivalent, $P_{th,curve}$, on the pumping curve using Q_{curve}. The pressure contribution due to the pump can be determined using the following equation.

$$P_{th} = P_{th,curve}\left(\frac{\omega}{\omega_{curve}}\right)^2\left(\frac{\rho_M}{\rho_{curve}}\right),\dots\dots\dots\dots\dots\dots\dots\dots\dots\dots\dots\dots\dots\dots\dots\dots.(A16)$$

where ρ_{curve} refers to the reference density in the centrifugal pump used to make the pumping curve. The

centrifugal pump used in this work is a high capacity pump that has the ability to increase the pressure of the nanoemulsion from the mixing stage. A synthetic pumping curve in conjunction with pump affinity relationships were used to describe the relationship between the pressure and flow rate for the centrifugal pump. The pumping curve used for this work is illustrated in **Figure 14**. Previously discussed pump affinity laws were used to scale the pumping curve for several impeller angular velocities. In addition, the pump had several more specifications listed in **Table 6**.
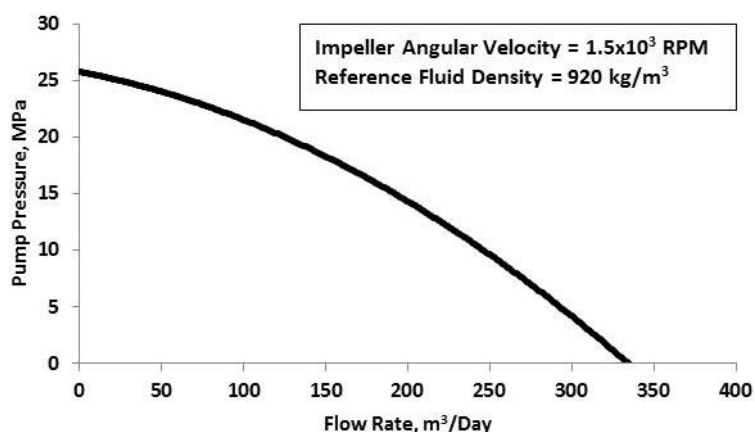

Figure 14—High capacity centrifugal pump curve.

Table 6—Centrifugal pump parameters.

Pump Impeller Diameter (Morales et al. 2013)	.231775 m
Fraction Turbulent Energy of Dissipation (Morales et al. 2013)	0.0019
Pump Active Volume	.05 m^3 (50 L)
Pump Impeller Angular Velocity	5000 RPM

Uchenna Odi is a Data Scientist at Devon Energy Corporation. He was previously a Research Scientist at ENI Petroleum and a Visiting Scientist at the Massachusetts Institute of Technology on behalf of ENI. He holds a B.S. degree in chemical engineering and an energy focused executive MBA both from the University of Oklahoma. He also holds M.S. and Ph.D. degrees in petroleum engineering from Texas A&M University. His interests are in optimization algorithms, risk analysis, emulsion systems, enhanced oil recovery, carbon dioxide sequestration, reservoir fluids, and machine learning.